Simple Method for the Real-Time Estimation of Timing Jitter in Ultrashort Pulses From Mode-Locked Ultralong Ring Fiber Lasers

Alejandro Rosado, Ines Cáceres-Pablo, and Juan Diego Ania-Castañón

***Abstract*—A simple method for the estimation of timing jitter in ultrafast lasers is presented and applied for the first time to the characterization of ultralong passively mode-locked femtosecond fiber oscillators with ultra-low repetition rates in the range of kHz. RMS jitter of the order of tens of fs is demonstrated, showing the potential of these recently introduced family of oscillators to be used in phase-noise sensitive applications.**

***Index Terms*—Mode-locked fiber lasers, soliton, timing jitter estimation.**

I. Introduction

A RECENT breakthrough in ultralong laser [1] technology was achieved with the introduction of a novel class of ultralong passively mode-locked femtosecond pulse fiber oscillators operating in the C-band at remarkably low repetition rates as low as 20 kHz [2], [3], [4]. The first iterations of these sources rely on Erbium-doped fiber amplifiers (EDFAs) and InN semiconductor saturable absorber mirrors (SESAMs), using quasi-solitonic propagation through an extended fiber ring to achieve multi-kilometric cavity lengths and low-cost generation of high-power femtosecond range pulses [5], [6]. Moreover, they do so without requiring any external stage or chirped-pulse amplification (CPA), paving the way for interesting applications such as supercontinuum generation and gas sensing [7]. This new family of lasers presents interest also from the point of view of mode-locking and pulse formation dynamics [8], [9], with the first studies demonstrating tunable harmonic mode-locking with apparent forbidden transitions [10].

The noise performance of ultrafast lasers has a strong impact on their potential applicability in multiple areas, especially those that are related with the generation of optical frequency combs (OFCs), the frequency counterpart of these high-power pulses. Noise can significantly affect to the laser linewidth and destabilize the frequency of each comb line, becoming highly relevant in metrological or spectroscopical applications, so it needs to be adequately measured or estimated. Noise in mode-locked lasers can manifest itself [11] in the form of intensity noise, mainly due to the fluctuations of the output power amplitude, or as frequency noise, arising from the frequency fluctuations of each comb line. Each comb line frequency fn is given by $f_n = f_{ceo} + n \cdot f_r$, where f_{ceo} is the carrier envelope frequency offset and fr the frequency separation between each comb line. When f_{ceo} fluctuates, the resulting noise is known as comb-line frequency noise. On the other hand, when it is the frequency separation that changes, the resulting noise is referred to as timing jitter, and can be easily observed in the temporal optical trace. Defined as the temporal fluctuation of the arriving time of successive optical pulses due to the variation of the frequency separation between the comb lines, its measurement in ultra-short optical pulses can be considerably challenging, mainly due to the intrinsically low level of timing jitter in femtosecond Mode-Locked ultralong ring fiber lasers. In the past, several methods have been developed to quantify the value of the timing jitter of ultra-short optical pulses generated in passive mode-locked lasers [12], [13], [14], [15]. Although some of them rely on simple techniques for the timing jitter retrieval, such as the characterization of the RF spectrum [12] or the use of external modulators [13], most of them rely on the use of balanced optical cross-correlators or optical heterodyning [14], [15]. All these methods require complex, highly specific, and expensive equipment.

In this letter we propose a simple alternative to estimate the timing jitter of the optical pulses generated by femtosecond Mode-Locked ultralong ring fiber lasers. In general terms, we have measured the temporal profile of several highly attenuated pulses traveling through a dispersive fiber spool under a dispersive regime. Then offline, the results are post-processed to compensate the dispersion induced by the fiber and calculating the temporal separation between the recompressed consecutive pulses, an experimental value of the timing jitter is obtained.

II. Estimative Method and Experimental Validation

This estimative method relies on the use of dispersive fiber to measure the optical pulses generated by the ultralong ring

Received 20 June 2024; revised 11 September 2024; accepted 19 September 2024. Date of publication 23 September 2024; date of current version 16 January 2025. This work was supported in part by MCIU/AEI/10.13039/501100011033 under Grant TED2021-131957B-100, Grant PID2021-1234590B-C21 and Grant PID2021-128000OB-C21, in part by the European Union NextGenerationEU/PRTR, and in part by ERDF "A Way of Making Europe". The work of Alejandro Rosado was supported by "Ayudas Margarita Salas para la formación de jovenes doctores" from Universidad Politécnica de Madrid, financed by European Union - NextGenerationEU. *(Corresponding author: Alejandro Rosado.)*

Alejandro Rosado is with the CEMDATIC - E.T.S.I. Telecomunicación, Universidad Politécnica de Madrid, 28040 Madrid, Spain (e-mail: alejandro.rosado@upm.es).

Ines Cáceres-Pablo and Juan Diego Ania-Castañón are with the Instituto de Oṕtica 'Daza de Valdes', IO-CSIC, C/Serrano 121, 28006 Madrid, Spain.

Color versions of one or more figures in this article are available at https://doi.org/10.1109/JLT.2024.3466240.

Digital Object Identifier 10.1109/JLT.2024.3466240

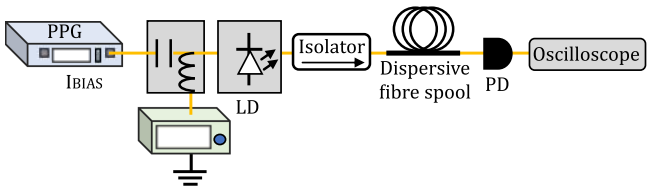

Fig. 1. Experimental setup for validation of the estimation method. LD: laser diode, OI: optical isolator, PPG: pulse pattern generator, PD: photodetector.

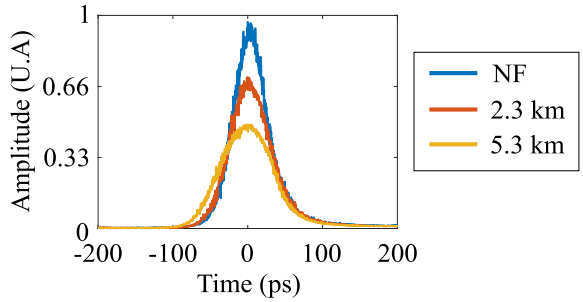

Fig. 2. Optical pulses generated by the GS-DML propagated through different lengths of dispersive fibers: no fiber (blue), 2.3 km (red) and 5.3 km (yellow).

fiber lasers with a known value of GVD. Then, the obtained pulses are post-processed offline to compensate the GVD pulse dispersion. To test the validation of this method, it has been applied to broader optical pulses, whose temporal width and timing jitter can be measured without dispersive fiber and usual instrumentation. Gain-switched (GS) optical pulses from a discrete mode laser (DML) have been chosen for this purpose. A scheme of the experimental setup for the method validation is displayed in Fig. 1.

A single-mode high-frequency DML at 1550 nm with a nominal modulation bandwidth of 10 GHz was gain-switched with a superposition of two electrical signals: a bias current of 10.9 mA and electrical pulses with a pulse duration of 200 ps, provided by a pulse pattern generator at a repetition rate of $f_R = 100$ MHz and a peak-to-peak amplitude of $V_{RF} = 1$ V. The temperature of the laser is controlled by a temperature controller. Then, the optical pulses are linearly dispersed by a fiber spool of ITU G.652 standard single-mode fiber of 2.3 and 5.3 km and measured with a digital scope analyzer with an optical input module with 20 GHz-bandwidth. The resulting pulses are shown in Fig. 2.

As it can be clearly seen in the pulses depicted in Fig. 2, the optical pulses generated in the GS laser diode exhibit a clear Gaussian profile, with a noticeable increase in the temporal full-width half-maximum (FWHM) alongside a decrease in the peak power of each pulse as the length of the dispersive fiber increases. A summary of the measured FWHM and the RMS timing jitter is shown in the Table I. The estimative method is performed as follows: since the pulses at the laser output pulses are not transform-limited, the auto-correlation trace profile is multiplied by a quadratic phase term, to consider for the final chirp at the end of the generation stage, obtaining an initial estimate for the optical field of the pulses. As it is previously shown in [16], during the most part of generation stage of the optical pulse, the instantaneous frequency chirp is linear, and therefore, the phase can be simplified.

TABLE I
MEASURED FWHM AND RMS TIMING JITTER OF THE MEASURED OPTICAL PULSES GENERATED IN THE GS-DML WITH DIFFERENT FIBER LENGTHS

Fiber length (m)	FWHM (ps)	RMS timing jitter (ps)
No fiber	48.5 ± 0.3	3.1 ± 0.3
2300	60 ± 0.3	4.3 ± 0.3
5300	78.5 ± 0.3	6.4 ± 0.3

TABLE II
CALCULATED FWHM AND RMS TIMING JITTER OF THE MEASURED OPTICAL PULSES GENERATED IN THE GS-DML WITH DIFFERENT FIBER LENGTHS USING THE ESTIMATIVE METHOD

Fiber length (m)	FWHM (ps)	RMS timing jitter (ps)
2300	48.2 ± 0.3	3.4 ± 0.3
5300	50.1 ± 0.3	3.5 ± 0.3

Besides, as the dispersion in the fiber is known, the initial estimate of the optical field is linearly propagated by multiplying by the GVD dispersion term of the non-linear Schrodinger equation:

$$\phi_{GVD}(L) = exp\left(\frac{i\beta\omega^2 L}{2}\right). \quad (1)$$

where β, ω represents the GVD coefficient and the frequency, respectively, and L the length of the fiber. The initial phase term at the output of the laser can then be calculated by iteratively adjusting the chirp parameter to get a close match between the pulses measured after dispersive broadening and their simulated counterparts. The phase of the dispersed field is then extracted and multiplied by the experimental measurements of the pulses, and after that, these are compressed by applying backpropagation with the reversed GVD dispersion term of the non-linear Schrodinger (1). Once all the pulses of the long temporal trace are backpropagated, they are represented together. The results of the estimative method over the GS-DML are graphically displayed in Fig. 3 and a summary of the obtained values for the RMS timing jitter is in the Table II.

The mean value of the temporal FWHM of the backpropagated pulses is close to the measured one of the original pulse (48.2 ps with the 2.3-km fiber and 50.1ps with the 5.3-km fiber), keeping the same shape of the original pulse (Fig. 2, in blue). Besides, the values of the RMS timing jitter obtained through this method are like the timing jitter of the optical pulse without fiber. The estimated values of the RMS timing jitter for the backpropagation of the optical pulses are presented in Table II. As can be extracted from Table II, the values of the RMS timing jitter provided by the estimative method of backpropagating optical pulses dispersed by dispersive fiber are like the ones extracted from the direct measurement of the RMS timing jitter of the non-dispersed optical pulse, thus evidencing of the effectiveness of the method.

III. TIMING JITTER ESTIMATION OF A FEMTOSECOND MODE-LOCKED ULTRALONG RING FIBER LASER

As it is demonstrated in the previous section, the backpropagation estimation method reliably determines the timing jitter of pulses propagating backwards along a dispersive fiber in its origin. This method can be applied over optical pulses

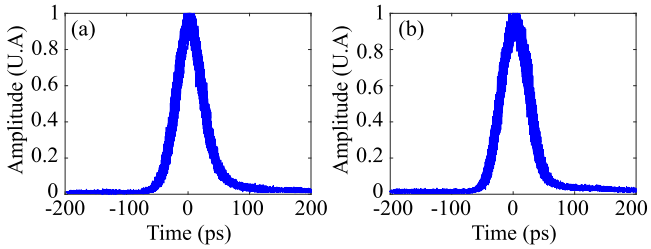

Fig. 3. superimposed profiles of 50 optical pulses generated with the GS-DML and backpropagated along a dispersive fiber of L = 2.3 km (a) and 5.3 km (b).

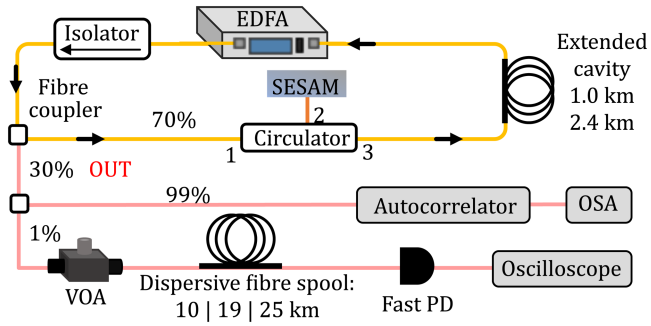

Fig. 4. Schematic of the setup for the characterization of ultralong pulsed fiber lasers, where the extended cavity and the dispersive fiber span can take different lengths. OSA: optical spectrum analyzer, VOA: variable optical attenuator.

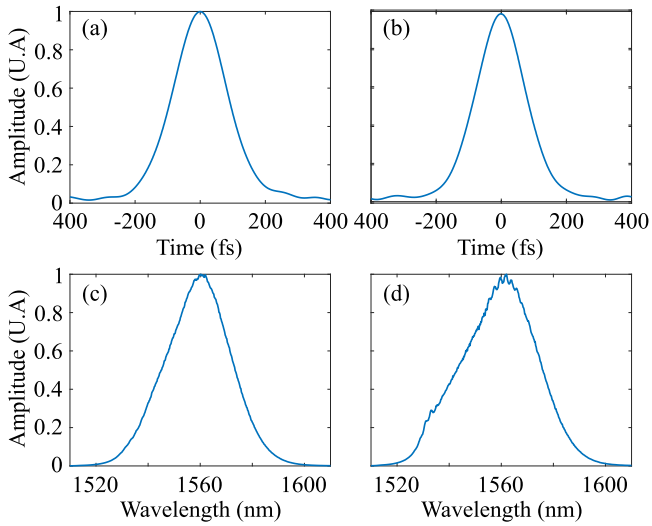

Fig. 5. Autocorrelation traces and optical spectra for: (a) and (b) the 1-km ring; and (c) and (d) the 2.4-km ring.

TABLE III
OBTAINED RESULTS FOR THE DISPERSION OF FIBER SPOOL WITH DIFFERENT LENGTHS

Fiber length (m)	Dispersion parameter (ps/nm·km)
10.250	17.80
18.890	22.50
25.250	12.10

whose temporal FWHM or their RMS timing jitter cannot be obtained through traditional approaches due to its short duration (less than 1 ps). As it is previously shown in [2], the optical pulses generated by a Femtosecond Mode-Locked Ultralong Ring Fiber Laser cannot be characterized with conventional instrumentation. Although the temporal FWHM and its shape can be measured with an autocorrelator, the timing jitter requires more advance (and expensive) instrumentation, and it would benefit from the simplicity of the estimative method.

A schematic depiction of our ultrafast ring fiber laser setup is shown in Fig. 4, where two stages can be clearly differentiated. The first stage is the laser itself. The laser includes a 16 m EDFA with a non-adjustable gain level at a fixed 24 dBm maximum output saturated power at 1560 nm. An InN semiconductor saturable absorber mirror, in free space configuration, resistant to high irradiances [4], [17], [18], polarization independent, coupled to the system through a circulator, capable of producing pulses in the order of femtoseconds is used to induce passive mode-locking by controlling the focus and spot size incident to the mirror. The extended cavity is placed after the SESAM and is constituted by a fiber spool of ITU G.652 standard single-mode fiber of 1 or 2.4 km. The system presents average anomalous dispersion and operates in the telecommunications C-band without external compression and amplification stages. The resulting pulses, generated by passive mode-locking, have pulse durations of the order of a few hundred femtoseconds and are characterized in the measurement stage. The laser output is divided by a 1:99 optical coupler. The light coming through the 99% output is temporally and spectrally characterized with an autocorrelator and an optical spectrum analyzer (OSA), respectively. The other branch is further attenuated to avoid non-linearities and sent through a dispersive fiber spool with different lengths (10, 19 and 25 km) and known group-velocity dispersion (GVD), and then, to a fast photodetector (nominal bandwidth 12 GHz) in conjunction with a real-time oscilloscope with an electrical bandwidth of 8 GHz and a maximum sampling rate of 20 Gbps/s.

The autocorrelation traces and the optical spectrum were measured in conditions of fundamental mode locking corresponding to repetition rates of 196 kHz and 89 kHz respectively (Fig. 5). The temporal full-width half-maximum (FWHM) of each pulse is 175 fs and 188 fs, and the peak power at the laser output are 28.5 mW and 27.62 mW for the 1 km cavity and for the 2.4 km ring, respectively. Both pulses are very similar in terms of shape and pulse width. In these systems, the pulse duration is primarily determined by the EDFA and SESAM, which remain the same for both cavities. Since the pulse intensity is adjusted at the SESAM to guarantee a nearly ideal solitonic propagation, the shape and duration of the pulses are preserved over the extended cavity. In the spectral domain, the optical spectra with the 1-km cavity have a spectral width at half maximum of 28 nm, whereas the other case with 2.4-km cavity is 32 nm. The value of the GVD dispersion parameter have been obtained by measuring each fiber spool with a GVD analyzer. All the obtained parameters are within the range of typical values and displayed in Table III. For both cases, we have measured the resulting output temporal pulses from our femtosecond Mode-Locked ultralong ring fiber laser, after attenuating the signal to guarantee dispersive

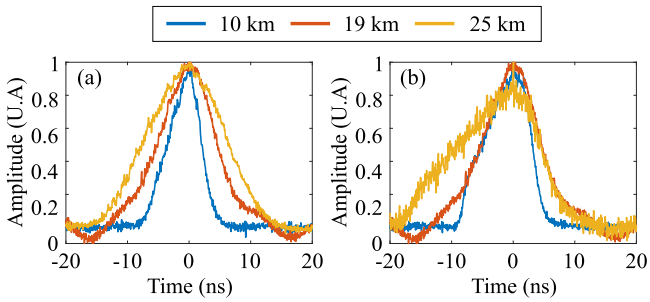

Fig. 6. Optical pulses generated by the femtosecond ultralong ring fiber laser propagated though different lengths of dispersive fibers: 10 km (blue), 19 km (red) and 25 km (yellow) and an extended cavity of (a) 1 km and (b) 2.4 km.

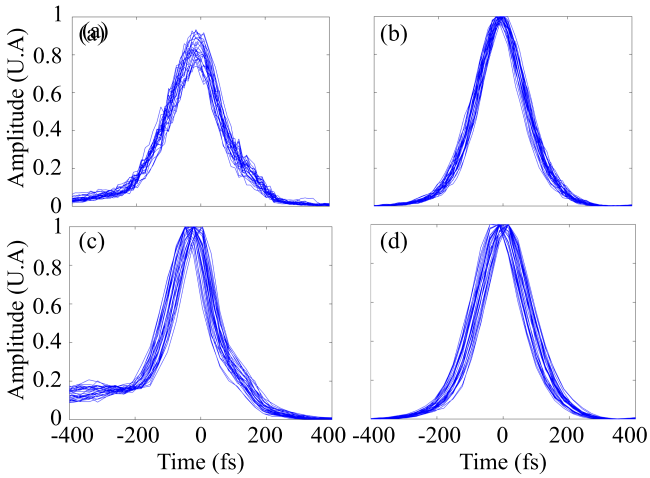

Fig. 7. Accumulated temporal traces of 80 optical pulses backpropagated along a dispersive fiber of L = 10 km and 25 km with: (a) and (b) the 1-km cavity; and (c) and (d) the 2.4-km cavity. All displayed temporal traces have been normalized by the maximum amplitude of Fig. 7(b).

broadening and propagating it through 3 fiber spools with different lengths: 10, 19 and 25 km., which is equivalent to performing a time stretch dispersive Fourier transform (TS-DFT) [19].

In the case of the 1-km ring, the corresponding values of the FWHM using a dispersive fiber of 10, 19 and 25 km are 6, 10 and 15 ns, respectively. In the second case, these values are 8, 10 and 15 ns. Note that the pulse shape of the broadened pulses generated by the 2.4-km cavity depicted on Fig. 6(b) is different from that of the pulses of Fig. 6(a), corresponding to the 1 km cavity. The pulses of the 2.4-km cavity are more affected by the presence of ASE noise from the EDFA, which modifies the optical spectrum, as seen on Fig. 5(d), which itself reflects on the temporal profile after the dispersive Fourier transform.

Despite this, both cavities generate pulses with similar temporal characteristics in terms of pulse-width and power. Here is where the estimative method is applied, to estimate timing jitter of the pulse generated by the ultralong ring laser in its source. Fig. 7 shows an accumulation of 80 optical pulses once the phase is corrected by (1) to compensate for the GVD.

After that, the resulting pulses have similar features and characteristics to the directly measured autocorrelation traces. In particular, the backpropagated pulses have an averaged FWHM of 185 fs, which is very close to the observed measured temporal

TABLE IV
PEAK TO PEAK TIMING JITTER (RMS) CALCULATED FROM THE MEASURED OPTICAL PULSES AT DIFFERENT FIBER LENGTHS AND EXTENDED CAVITIES

Fiber length (m)	1-km cavity (fs)	2.4-km cavity (fs)
10.250	30 (12) ± 5	49 (33) ± 5
18.890	46 (37) ± 5	55(39) ± 5
25.250	34 (19) ± 5	58(44) ± 5

FWHM with the autocorrelator. Besides, all backpropagated pulses have a strong hyperbolic sech component, being highly symmetric and with a high degree of resemblance to the original autocorrelation traces.

From the compressed, backpropagated trace, we can calculate the peak-to-peak timing jitters at half maxima, which are summarized on Table IV. Considering all the results, no correlation seems to exist between the corrected timing jitters and the length of the dispersive fiber spool. However, there are some visible differences between the calculated values of timing jitter using two different extended cavities. In the case of the 1-km extended cavity, the average time jitter for the three fiber spools is 23 fs, whereas when the other cavity is employed, the value of the averaged timing jitter is higher, 39 fs. This is to be expected, as longer cavities present lower repetition rates, a higher ASE noise level and larger overall cavity length fluctuations due to environmental factors, all of which will have a direct influence on the measured timing jitter and phase noise.

IV. CONCLUSION

Here, we present a very simple algorithm to estimate the timing jitter of optical pulses generated by ultra-long ring fiber lasers with simple equipment that can be found in any optical communication laboratory and apply it to the estimation of timing jitter in ultralong pulsed fiber lasers. The method consists of measuring the ultra short optical pulses produced by our lasing source after they propagates along a dispersive fiber spool with a known length, to properly characterize the broader optical pulse with standard instrumentation and enough resolution. After that, the complex amplitude is multiplied by a corrective phase that compensates the effect of the GVD dispersion. The timing jitter has been obtained from the accumulated several compensated optical pulses. The results provided by our experimental study show that this method is perfectly able to retrieve consistent and coherent estimations of the timing jitter in different experimental scenarios. The low jitter values obtained for our ultralong laser setups also showcases their potential use in applications in which phase noise could pose an important limitation. Finally, we confirm a direct correlation between cavity length and timing jitter in ultralong ring fiber lasers, as it can be expected from increased ASE and cavity length fluctuations.

ACKNOWLEDGMENT

The authors wish to thank Profs. E. Monroy, F. B. Naranjo, and M.González-Herráez for providing the InN samples employed in the SESAM, Profs. I. Esquivias and J.M.G. Tijero for the optical instrumentation employed for the laser diode characterization and Dr. P. Corredera for providing critical fiber equipment.

REFERENCES

[1] J. D. Ania-Castañón, T. J. Ellingham, R. Ibbotson, X. Chen, L. Zhang, and S. K. Turitsyn, "Ultralong Raman fiber lasers as virtually lossless optical media," *Phys. Rev. Lett.*, vol. 96, no. 2, Jan. 2006, Art. no. 023902.

[2] I. Cáceres-Pablo, F. Gallazzi, F. Solís, P. Corredera, and J. D. Ania-Castañón, "Ultralong passively mode-locked ring fibre lasers in the femtosecond range assisted by Raman amplification," *Opt. Laser Technol.*, vol. 166, Nov. 2023, Art. no. 109562.

[3] F. Gallazzi et al., "Sub-250 fs passively mode-locked ultralong ring fibre oscillators," *Opt. Laser Technol.*, vol. 138, Jun. 2021, Art. no. 106848.

[4] M. Jiménez-Rodríguez, E. Monroy, M. González-Herráez, and F. B. Naranjo, "Ultrafast fiber laser using inn as saturable absorber mirror," *J. Lightw. Technol*., vol. 36, no. 11, pp. 2175–2182, Jun. 2018. [Online]. Available: https://opg.optica.org/jlt/abstract.cfm?URI=jlt-36-11-2175

[5] I. Cáceres-Pablo and J. D. Ania-Castañón, "Real-time transition dynamics of harmonically mode-locked femtosecond ultralong ring fiber lasers," in *2022 Eur. Conf. Opt. Commun.*, 2022, pp. 1–3.

[6] I. Cáceres-Pablo and J. D. Ania-Castañón, "Impact of polarization and gain control in the optimization of output pulse properties in ultralong ultrafast ring fibre lasers," *Results Phys.*, vol. 64, 2024, Art. no. 107936.

[7] F. Gallazzi et al., "Ultralong ring laser supercontinuum sources using standard telecommunication fibre," *Opt. Laser Technol.*, vol. 147, Mar. 2022, Art. no. 107632.

[8] X. Liu, X. Yao, and Y. Cui, "Real-time observation of the buildup of soliton molecules," *Phys. Rev. Lett.*, vol. 121, no. 2, 2018, Art. no. 023905.

[9] X. Liu and M. Pang, "Revealing the buildup dynamics of harmonic mode-locking states in ultrafast lasers," *Laser Photon. Rev.*, vol. 13, 2019, Art. no. 1800333.

[10] I. Cáceres-Pablo and J. D. Ania-Castañón, "Real-time transition dynamics of harmonically mode-locked femtosecond ultralong ring fiber lasers," *J. Lightw. Technol.*, vol. 42, no. 13, pp. 4643–4649, Jul. 2024.

[11] J. Kim and Y. Song, "Ultralow-noise mode-locked fiber lasers and frequency combs: Principles, status, and applications," *Adv. Opt. Photon.*, vol. 8, no. 3, Aug. 2016, Art. no. 465.

[12] D. von der Linde, "Characterization of the noise in continuously operating mode-locked lasers," *Appl. Phys. B*, vol. 39, no. 4, pp. 201–217, Apr. 1986.

[13] Hewlett Packard Company, "Phase noise characterization of microwave oscillators (product note 11729 C-2)," 1985.

[14] Y. Song, K. Jung, and J. Kim, "Impact of pulse dynamics on timing jitter in mode-locked fiber lasers," *Opt. Lett.*, vol. 36, no. 10, May 2011, Art. no. 1761.

[15] D. Hou, C.-C. Lee, Z. Yang, and T. R. Schibli, "Timing jitter characterization of mode-locked lasers with < 1 zs / $\sqrt{hz}$ resolution using a simple optical heterodyne technique," *Opt. Lett.*, vol. 40, no. 13, Jun. 2015, Art. no. 2985.

[16] A. Rosado, A. Perez-Serrano, J. M. G. Tijero, A. V. Gutierrez, L. Pesquera, and I. Esquivias, "Numerical and experimental analysis of optical frequency comb generation in gain-switched semiconductor lasers," *IEEE J. Quantum Electron.*, vol. 55, no. 6, Dec. 2019, Art. no. 2001012.

[17] A. J. DeMaria, D. A. Stetser, and H. Heynau, "Self mode-locking of lasers with saturable absorbers," *Appl. Phys. Lett.*, vol. 8, no. 7, pp. 174–176, Apr. 1966.

[18] H. A. Haus, "Theory of mode locking with a fast saturable absorber," *J. Appl. Phys.*, vol. 46, no. 7, pp. 3049–3058, Jul. 1975.

[19] K. Goda and B. Jalali, "Dispersive fourier transformation for fast continuous single-shot measurements," *Nature Photon.*, vol. 7, no. 2, pp. 102–112, Jan. 2013.